Bioelectrochemistry 147 (2022) 108205

Contents lists available at ScienceDirect

Bioelectrochemistry

journal homepage: www.journals.elsevier.com/bioelectrochemistry

Low-frequency repetitive magnetic stimulation suppresses neuroblastoma progression by downregulating the Wnt/β-catenin signaling pathway

Seongmoon Jo [a,b,1], Sang Hee Im [a,1], Dongryul Seo [c], Hayeon Ryu [c], Sung Hoon Kim [d], Dawoon Baek [d], Ahreum Baek [d,*], Sung-Rae Cho [a,b,e,f,*]

[a] Department and Research Institute of Rehabilitation Medicine, Yonsei University College of Medicine, Seoul, South Korea
[b] Brain Korea 21 PLUS Project for Medical Science, Yonsei University College of Medicine, Seoul, South Korea
[c] Department of Medicine, Yonsei University College of Medicine, Seoul, South Korea
[d] Department of Rehabilitation Medicine, Yonsei University Wonju College of Medicine, Wonju, South Korea
[e] Graduate Program of Biomedical Engineering, Yonsei University College of Medicine, Seoul, South Korea
[f] Rehabilitation Institute of Neuromuscular Disease, Yonsei University College of Medicine, Seoul, South Korea

ARTICLE INFO

Keywords:
Repetitive magnetic stimulation
Low-frequency
Neuroblastoma
Wnt/β-catenin signaling pathway
Tumor suppression effect

ABSTRACT

Repetitive magnetic stimulation (rMS) has been suggested as a non-invasive treatment for various neurological or psychiatric diseases. Contrary to the application previously used, the purpose of the present study was to elucidate whether low-frequency rMS could suppress tumor progression in *in vitro* and *in vivo* neuroblastoma models, and to explore the underlying mechanisms. The results demonstrated that low-frequency rMS treatment significantly suppressed cell proliferation and tumor progression in the models. Moreover, low-frequency rMS treatment downregulated the Wnt/β-catenin signaling pathway and induced apoptosis. The Wnt/β-catenin signaling pathway activator, Wnt agonist, was found to counteract the effect of low-frequency rMS treatment, while the Wnt/β-catenin signaling pathway inhibitor, Wnt antagonist, exhibited a tumor suppression effect, similar to the effect of low-frequency rMS treatment. Taken together, our data demonstrated that low-frequency rMS treatment suppressed neuroblastoma progression by downregulating the Wnt/β-catenin signaling pathway, suggesting that low-frequency rMS treatment may be a potential therapeutic strategy for the tumor suppression.

1. Introduction

Magnetic stimulation (MS) is a non-invasive treatment for delivering electrical stimuli and producing magnetic flux in nervous tissue through neuronal depolarization [1]. Generally, single-pulse MS is used to explore brain function, whereas repetitive magnetic stimulation (rMS) with a regular frequency is used to control the excitability of brain regions [2]. Since rMS is a non-invasive and less painful treatment with no side effects, many studies have reported the use of rMS as a therapy for various disorders, such as psychiatric dysfunction, Parkinson's disease, stroke, and pain syndromes [3]. The excitability of brain regions can be increased or decreased depending on the frequency, intensity, and pattern of rMS [4,5]. rMS frequency is considered to be the primary determinant of differential effects in various types of diseases [6]. Generally, clinical rMS has been classified as high-frequency (>5 Hz) and low-frequency (≤1 Hz) [7–9]. High-frequency stimulation has an excitatory effect, whereas low-frequency stimulation has an inhibitory effect [10,11]. Depending on the frequency of stimulation, rMS could be

Abbreviations: MS, Magnetic stimulation; rMS, Repetitive magnetic stimulation; N2a, Neuro-2a; DMEM, Dulbecco's modified Eagle's medium; FBS, Fetal bovine serum; OD, Optical density; CCK-8 assay, Cell counting kit-8 assay; CFA, Colony formation assay; RNA-seq, RNA Sequencing; GO, Gene ontology; DAVID, Database for annotation, visualization and integrated discovery; PI3K, Phosphatidylinositol-4,5-bisphosphate 3-kinase; ERK, Extracellular signal-regulated kinase; JNK, c-Jun N-terminal kinase; AKT, AKT Serine/Threonine kinase; mTOR, Mechanistic target of rapamycin; WNT3α, Wnt family member 3A; WNT5α, Wnt family member 5A; DVL1, Dishevelled segment polarity protein 1; GSK3β, Glycogen synthase kinase 3 beta; LEF1, Lymphoid enhancer binding factor 1; Bax, Bcl-2 associated X, apoptosis regulator; Bcl-2, B-cell lymphoma 2; TUNEL, Terminal dUTP Nick End-Labeling; TMZ, Temozolomide; DEGs, Differentially expressed genes; mT, millitesla.

* Corresponding authors at: Department of Rehabilitation Medicine, Yonsei University Wonju College of Medicine, 20 Ilsan-ro, Wonju-si, Gangwon-do 26426, South Korea (A. Baek). Department and Research Institute of Rehabilitation Medicine, Yonsei University College of Medicine, 50 Yonsei-ro, Seodaemun-gu, Seoul, 03722, South Korea (S.-R. Cho).
E-mail addresses: ahreumbaek@yonsei.ac.kr (A. Baek), srcho918@yuhs.ac (S.-R. Cho).
[1] These authors contributed equally to this work.

https://doi.org/10.1016/j.bioelechem.2022.108205
Received 8 March 2022; Received in revised form 31 May 2022; Accepted 5 July 2022
Available online 9 July 2022

utilized for many neurological diseases [12].

Neuroblastoma is an embryonic cancer of the nervous system derived from the neural crest [13]. Upon diagnosis with neuroblastoma, the patients are mostly classified as high-risk neuroblastoma because its presentation is highly variable, including benign tumors and substantial tumor metastasis that leads to major illnesses [14]. For neuroblastoma treatment, currently, chemotherapy is used to shrink the primary tumor size and reduce the possibility of metastases along with radiation or surgery [15]. Even though significant advances in patient outcomes have been accomplished with the combination of conventional treatments, highly aggressive treatments such as chemotherapy, surgery, and radiation are major burdens for patients [16]. Moreover, long-term follow-up treatment and possible complications, including cardiac dysfunction, infertility, and regional recurrence, represent risks to patients after primary treatment [17]. Therefore, it is important to develop more effective and less toxic therapies to improve the survival of patients [18].

Recently, rMS has been suggested as a non-invasive treatment for cancer patients to treat their chronic pain and depression by targeting motor cortex stimulation [19,20]. Moreover, rMS is used as a method for brain imaging because it provides functional information through direct stimulation of brain regions [21]. It is performed prior to brain tumor surgery and generates active cartography of functional regions of the brain and minimizes craniotomy size [22,23]. Additionally, rMS may have an effect on tumor progression via suppression of tumor-development processes and stimulation of immune functions [24,25].

In previous studies, our group identified that low-frequency rMS reduces cell proliferation, while high-frequency rMS increases cell proliferation [26–28]. Therefore, in this study, we investigated the application of low-frequency rMS in neuroblastoma as a therapeutic treatment and the therapeutic mechanisms related to low-frequency rMS.

2. Materials and methods

2.1. Cell culture

The Neuro-2a (N2a) cell line (RRID: CVCL_0470) was purchased from the American Type Culture Collection. N2a cells were incubated in culture dishes with Dulbecco's modified Eagle's medium (DMEM) containing 10% fetal bovine serum (FBS) and 1% penicillin/streptomycin, in a humidified 5% CO_2 atmosphere at 37°C. The medium was replaced at three-day intervals. N2a cells were sub-cultured when they reached 80%–90% confluence. Trypsin-EDTA solution was used to dissociate the cells. All experiments were performed with mycoplasma-free cells.

2.2. Repetitive magnetic stimulation

In each experiment, the growth medium for N2a cells was replaced before stimulation. N2a cells were then stimulated with customized rMS (Bicon-1000Pro, Mcube Technology, Seoul, Korea). The intensity of stimulation was set to 18 mT (millitesla) and the stimulation delivered a monophasic pulse with a rise time of 370 μs. The frequency and amplitude of the stimulation were monitored with a probe connected to a digital multimeter and an oscilloscope as we described in previous studies [27,28]. N2a cells were stimulated by rMS during 3 d for 10 min/d. The distance between the center of the magnetic coil (70 mm diameter) and the culture dish was approximately 1.0 cm. The magnetic coil did not generate the heat during stimulation since a functional thermal sensor and a cooling system were implanted in the customized rMS. N2a cells were divided into two groups: sham group (emplacing culture dishes without rMS) and low-frequency group (0.5 Hz stimulation, on–off interval of 3 s). After rMS, N2a cells were harvested after Trypsin-EDTA disassociation.

2.3. Drug treatment

To clarify the effect of rMS on the Wnt/β-catenin signaling pathway, Wnt agonist 1 (Selleckchem, Houston, TX, USA) and XAV939 (Sigma Aldrich, St. Louis, MO, USA) were administered to N2a cells. Wnt agonist 1 (Wnt agonist) and XAV939 (Wnt antagonist) were administered at a concentration of 5 ng/ml for each dish before rMS over the course of 3 d. N2a cells were divided into six groups as follows: sham + vehicle group (treated with PBS), low-frequency + vehicle group (treated with rMS and PBS), sham + agonist group (treated with Wnt agonist 1), low-frequency + agonist group (treated with rMS and Wnt agonist 1), sham + antagonist group (treated with XAV939), and low-frequency + antagonist group (treated with rMS and XAV939).

2.4. Cell counting Kit-8 (CCK-8 assay)

CCK-8 assay was performed according to the manufacturer's instructions (Dojindo, Kumamoto, Japan). N2a cells were seeded into 96-well plates. After treatment, 10 μl of the kit reagent was added to each well. After incubation at 37°C for 1 h, optical density (OD) at 450 nm was measured using a multifunction microplate reader (VersaMax, Molecular Devices, San Jose, CA, USA) [29].

2.5. Colony formation assay (CFA)

For CFA, N2a cells were seeded into 6-well plates. For 10 d, N2a cells were incubated without sub-culturing. After fixation in 4% paraformaldehyde, N2a cells were stained with 0.4% Trypan blue. We counted visible colonies that contained at least 50 cells.

2.6. RNA preparation

After *in vitro* and *in vivo* experiments, total RNA was isolated according to the manufacturer's instructions. TRIzol (Thermo Fisher Scientific, Waltham, MA, USA) was used for RNA isolation [30]. A NanoDrop spectrophotometer (Thermo Fisher Scientific) was used to confirm RNA quantity and purity.

2.7. RNA sequencing (RNA-seq) transcriptome analysis

RNA-seq transcriptome analysis between sham group and low-frequency group was conducted at Macrogen Inc., (Seoul, Korea) using the HiSequation 2000 platform (Illumina, San Diego, CA, USA) for comparative analysis, as per methods described in previous studies [31].

2.8. Bioinformatics analysis

Gene ontology (GO) analysis of the identified genes was conducted using the Database for Annotation, Visualization and Integrated Discovery (DAVID) v.6.8 annotation tool to identify the role of genes. GO annotation of the genes was performed according to the associated biological processes. Organized assemblies for molecular function were described by each biological process [32].

2.9. Quantitative real-time reverse transcription-polymerase chain reaction

Quantitative real-time reverse transcription-polymerase chain reaction (RT-qPCR) was performed to validate the results of transcriptome analysis. According to the manufacturer's instructions, ReverTra Ace® qPCR RT Master Mix with gDNA Remover (Toyobo, Osaka, Japan) was used to prepare cDNA from total RNA. RT-qPCR to measure the mRNA levels of the genes of interest was performed using qPCRBIO SyGreen Mix Hi-ROX (PCR BIOSYSTEMS, London, UK) in a StepOnePlus Real-Time PCR System (Applied Biosystems, Foster City, CA, USA). The $2^{-\Delta\Delta}$CT method was used to conduct data analysis [33]. Supplementary

Table S1 described the primers used for RT-qPCR.

2.10. Western blot

After *in vitro* and *in vivo* experiments, proteins were extracted. Samples were boiled for 10 min and loaded onto NuPage 4%–12% bis-Tris gels (Invitrogen, Waltham, MA, USA). Separated proteins were blotted onto polyvinylidene difluoride membranes (Invitrogen) with 20% (v/v) methanol in NuPage Transfer Buffer (Invitrogen) at 15 V for 4 h at 4°C. Tris-buffered saline containing 0.01% Tween 20 (TBST) with 5% skim milk (Difco, BD Biosciences, Oxford, UK) was used to block membranes for 1 h. Blots were washed three times with TBST for 10 min, then incubated overnight at 4°C with primary antibodies specific for the following target proteins: phosphorylated PI3K (1:1000; Cell Signaling Technology, Cambridge, England), ERK, phosphorylated ERK, JNK, phosphorylated JNK, p38, phosphorylated p38, AKT, phosphorylated AKT, PI3K, mTOR, phosphorylated mTOR, WNT3α, WNT5α, DVL1, GSK3β, phosphorylated GSK3β, β-catenin, LEF1, cyclin D1, c-Myc, Bax, Bcl-2 and β-actin (1:1000; Santa Cruz Biotechnology, Santa Cruz, CA, USA). After incubation, blots were washed three times with TBST and incubated for 1 h with horse-radish peroxidase–conjugated secondary antibody (1:3000; Santa Cruz) at room temperature. Blots were visualized using an enhanced chemiluminescence detection system (Amersham Pharmacia Biotech, Little Chalfont, UK).

2.11. Ethics statement

The Association for Assessment and Accreditation of Laboratory Animal Care (AAALAC) and the Institutional Animal Care and Use Committee (IACUC) of Yonsei University Health System (permit number: 2020–0065) reviewed and approved the experiments of the study. All experiments were performed in accordance with the guidelines of the National Institutes of Health's Guide for the Care and Use of Laboratory Animals. These regulations, notifications, and guidelines originated and were modified from the Animal Protection Law (2008), the Laboratory Animal Act (2008), and the Eighth Edition of the Guide for the Care and Use of Laboratory Animals (NRC 2011). Mice were provided food and water ad libitum under a 12-h light/dark cycle, according to animal protection regulations. Animals were sacrificed after experiments by CO_2 inhalation. Our group made maximum efforts to minimize animal suffering.

2.12. In vivo xenograft model

To establish an *in vivo* neuroblastoma mouse model, 5×10^6 N2a cells suspended in 100 μl PBS were inoculated subcutaneously into the right hind limb anterior root of BALB/c nude mice (6–8 weeks old, male). After one week, mice with tumor over 50 mm^3 were selected and randomly allocated to each group. Mice in sham group received an equivalent dose of drug vehicle (PBS) and were placed in a modified restrainer, which contains an open space for the exposure of tumor mass to the coil of rMS in order to treat low-frequency rMS directly [34]. Mice in low-frequency group were placed in the modified restrainer and the magnetic coil was placed on the open space of the restrainer. The distance between the center of coil and the tumor mass was as approximately 1.0 cm to generate the same effect of rMS treatment with the *in vitro* experiment [35]. Then, mice were treated daily with 0.5 Hz rMS for 10 min over the duration of the experiment. Mice in TMZ group were treated daily with 30 mg/kg temozolomide (Sigma Aldrich). Mice in agonist group were treated daily with 5 mg/kg of Wnt agonist 1. Mice in antagonist group were treated daily with 5 mg/kg of XAV939. The tumor size in each xenograft model was measured daily. Approximately 18 d after the first treatment, all mice were euthanized, and the tumor masses were carefully removed.

2.13. Immunohistochemistry (IHC)

The tumor masses, removed from the *in vivo* neuroblastoma model, were fixed in 4% paraformaldehyde, embedded in paraffin, and cut into 3.5–4 μm thick sections. The sections were stained with an antibody against Ki-67 (1:400; Abcam, Cambridge, England), DVL1, and LEF1 (1:50; Santa Cruz Biotechnology). In addition, haematoxylin and eosin (H&E) staining was performed on these tissues using a standard staining protocol (Sigma Aldrich, St. Louis, USA).

2.14. Terminal dUTP Nick End-Labeling (TUNEL) assay

For analysis of apoptosis, N2a cells were seeded in a cell culture slide (30104, SPL Life Sciences, Gyeonggi-do, Korea). Low-frequency and drug treatments were performed as described in Cell Culture. Cell culture slides were fixed in 4% paraformaldehyde. For tumor masses of *in vivo* neuroblastoma model, the sections were prepared as described in IHC. After then, the DeadEnd™ Fluorometric TUNEL System (Promega, Madison, WI, USA) was conducted according to the manufacturer's protocol. Samples were mounted on glass slides with fluorescent mounting medium with DAPI for imaging, using the LSM 700 fluorescence microscope (Carl Zeiss, Gottingen, Germany). The number of positively stained cells over the total number of cells per specimen field was measured, and the percentage of positive cells was calculated. Four individual specimens per group were analyzed.

2.15. Statistical analysis

All data are expressed as means ± standard error of the mean (SEM), and all experiments were repeated at least four times with four technical replicates in each group. The Statistical Package for Social Sciences v.25.0 (IBM Corp. Released 2015. IBM SPSS Statistics for Windows, v.25.0. Armonk, NY, USA) was used for statistical analyses. The significance of intergroup differences was estimated using Student's paired *t*-test, one-way analysis of variance (ANOVA), or two-way ANOVA, as appropriate. Statistical significance was set at $P < 0.05$.

3. Results

3.1. Low-frequency rMS regulates cell proliferation in neuroblastoma

Cell proliferation and colony formation were assessed using the CCK-8 assay and CFA to evaluate the effect of low-frequency rMS. The *in vitro* neuroblastoma model was divided into two groups: sham group, which was not treated, and low-frequency group, which was treated with low-frequency rMS. In the CCK-8 assay, low-frequency group showed a significantly decreased proliferative rate compared to sham group (Fig. 1A-B). CFA revealed that colony formation was notably decreased after low-frequency rMS treatment (Fig. 1C-D). We then assessed the impact of low-frequency rMS on the JNK/p38/ERK and PI3K/AKT/mTOR pathways, which are related to unlimited cell proliferation, dedifferentiation, and a lack of tumor apoptosis [36,37]. Western blot results showed that the levels of phosphorylated JNK, p38, ERK, PI3K, AKT, and mTOR were significantly decreased after low-frequency rMS, indicating that the JNK/p38/ERK and PI3K/AKT/mTOR signaling pathways were significantly inactivated (Fig. 1E-H). These results suggested that low-frequency rMS inhibited cell proliferation and induced apoptosis in the *in vitro* neuroblastoma model.

3.2. Genes related to the Wnt/β-catenin signaling pathway are differentially expressed in neuroblastoma after low-frequency rMS treatment

RNA-seq transcriptome analysis was performed to identify DEGs in sham group and low-frequency group. In low-frequency group, 21,567 genes were differentially expressed compared to that in sham group; the

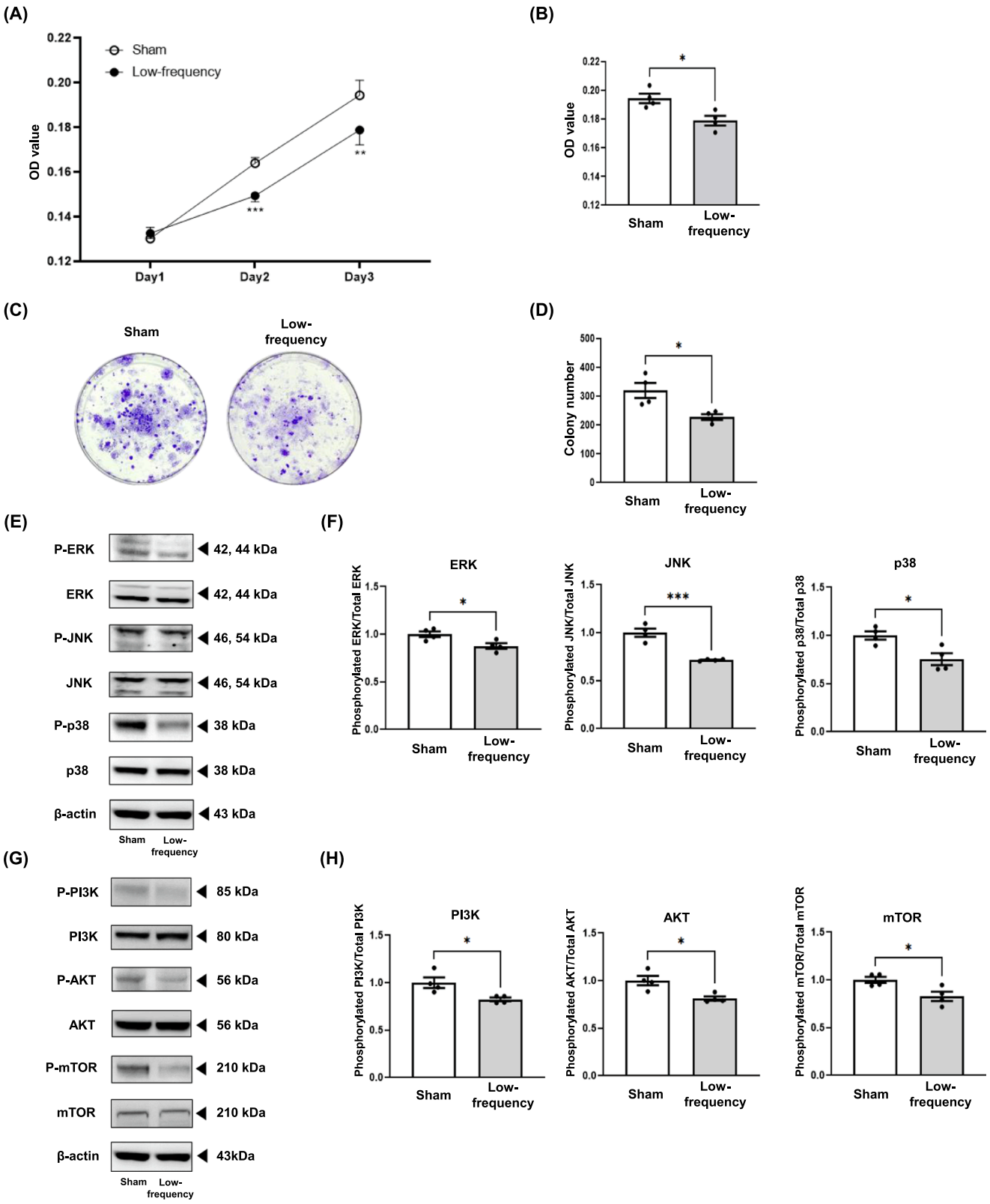

Fig. 1. Low-frequency rMS modulates cell proliferation in an *in vitro* neuroblastoma model. The model was divided into two groups: sham group (non-treated, n = 4) and low-frequency group (treated with low-frequency rMS, n = 4). (A) Cell counting kit-8 (CCK-8) assay of the *in vitro* neuroblastoma model treated with or without low-frequency rMS. (B) Quantification of CCK-8 assay. (C) Colony formation assay (CFA) of the *in vitro* neuroblastoma model treated with or without low-frequency rMS. (D) Quantification of CFA. (E) Western blot analysis of ERK, JNK, and p38 in the *in vitro* neuroblastoma model treated with or without low-frequency rMS. (F) Quantification of Western blot signals for ERK, JNK, and p38 (G) Western blot analysis of PI3K, AKT, and mTOR in the *in vitro* neuroblastoma model treated with or without low-frequency rMS. (H) Quantification of Western blot signals for PI3K, AKT, and mTOR. Values are presented as means ± standard error of the mean (SEM). Statistically significant differences are shown as *P < 0.05, **P < 0.01, ***P < 0.001.

expression of 407 transcripts and 429 transcripts was 1.5-fold higher and 1.5-fold lower, respectively, in low-frequency group than in sham group. GO analyses of biological processes with downregulated genes in low-frequency group were performed using the DAVID program (Fig. 2A and Supplementary Table 2). Biological processes are presented in the table and the figure based on the adjusted P-value [32]. Among the biological processes with downregulated genes in low-frequency group, we focused on the Wnt/β-catenin signaling pathway, which is highly related to cancer development and progression of neuroblasoma [38]. In addition, the GO terms for biological process, including DVL1 and LEF1, which play a major role in Wnt/β-catenin signaling cascades, were significantly downregulated after low-frequency rMS [39]. Therefore, we investigated and validated the Wnt/β-catenin signaling pathway as a potential mechanism for the tumor suppression effect of low-frequency rMS.

3.3. *Low-frequency rMS inhibits cell proliferation via downregulating the Wnt/β-catenin signaling pathway in an in vitro neuroblastoma model*

To validate the effect of low-frequency rMS on the Wnt/β-catenin

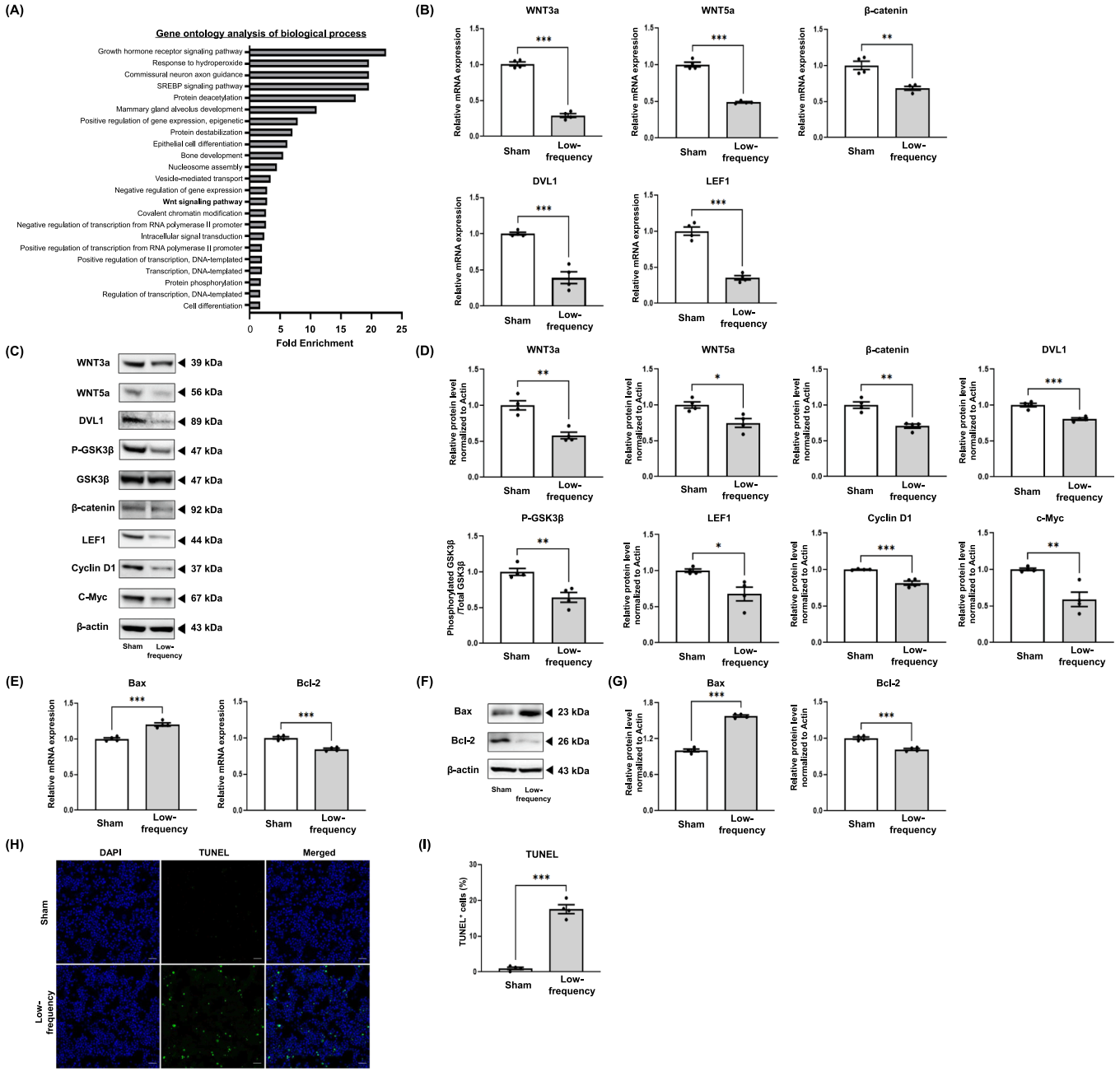

Fig. 2. Low-frequency rMS suppresses the cell proliferation via downregulating the Wnt/β-catenin signaling pathway in an *in vitro* neuroblastoma model. The model was divided into two groups: sham group (non-treated, n = 4) and low-frequency group (treated with low-frequency rMS, n = 4). (A) Gene ontology analysis of biological process downregulated by low-frequency rMS in neuroblastoma (B) The relative gene expression of WNT3a, WNT5a, β-catenin, DVL1, and LEF1 detected by RT-qPCR. (C) Western blot analysis of the Wnt/β-catenin signaling pathway in the *in vitro* neuroblastoma model treated with or without low-frequency rMS. (D) Quantification of Western blot signals for the Wnt/β-catenin signaling pathway (E) The relative gene expression of Bax and Bcl-2 detected by RT-qPCR (F) Western blot analysis of Bax and Bcl-2 in the *in vitro* neuroblastoma model treated with or without low-frequency rMS. (G) Quantification of Western blot signals of Bax and Bcl-2 (H) TUNEL assay in the *in vitro* neuroblastoma model treated with or without low-frequency rMS. (I) Quantification of TUNEL assay. Values are presented as means ± SEM. Statistically significant differences are shown as *P < 0.05, **P < 0.01, ***P < 0.001.

signaling pathway and apoptosis in neuroblastoma, RT-qPCR, Western blot, and TUNEL assay were conducted. The expression of the genes related to the Wnt/β-catenin signaling pathway, such as WNT3a, WNT5a, β-catenin, DVL1, and LEF1 was downregulated in low-frequency group compared to that in sham group (Fig. 2A). The expression of WNT3a, WNT5a, β-catenin, DVL1, LEF1, cyclin D1, and c-Myc was validated by Western blot, and after low-frequency rMS, their expression was downregulated. β-actin was used as an internal control. Phosphorylation of GSK3β was downregulated in low-frequency group compared to that in sham group (Fig. 2B-C). In addition, the expression gene and protein levels of anti-apoptotic marker, Bcl2 were down-regulated after low-frequency rMS while the expression levels of pro-apoptotic marker, Bax were upregulated (Fig. 2E-G). Moreover, TUNEL positive cells were increased in low-frequency group compared to that in sham group (Fig. 2H-I).

To further explore the effect of low-frequency rMS on the Wnt/β-catenin signaling pathway and apoptosis in neuroblastoma, Wnt agonist and antagonist were used in the *in vitro* neuroblastoma model. Wnt agonist and antagonist were administered to the *in vitro* neuroblastoma model with or without low-frequency rMS. Therefore, the *in vitro* neuroblastoma model was divided into six groups: sham + vehicle group (treated with PBS), low-frequency + vehicle group (treated with rMS and PBS), sham + agonist group (treated with Wnt agonist 1), low-frequency + agonist group (treated with rMS and Wnt agonist 1), sham + antagonist group (treated with XAV939), and low-frequency + antagonist group (treated with rMS and XAV939). The CCK-8 assay and

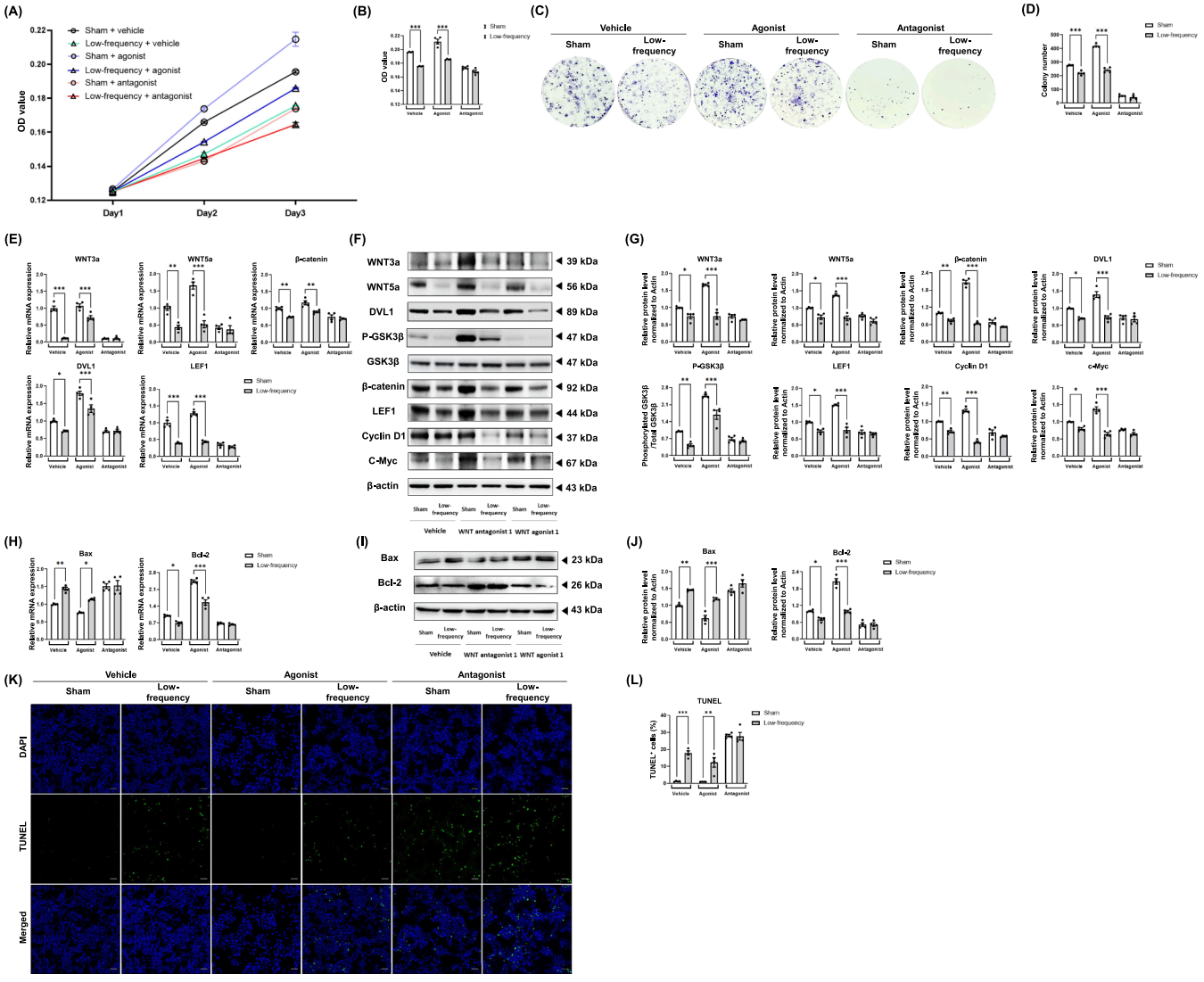

Fig. 3. Agonist and antagonist of the Wnt/β-catenin signaling pathway validated the effect of low-frequency rMS on the Wnt/β-catenin signaling pathway. The model was divided into six groups: sham + vehicle group (treated with PBS, n = 4), low-frequency + vehicle group (treated with rMS and PBS, n = 4), sham + agonist group (treated with Wnt agonist 1, n = 4), low-frequency + agonist group (treated with rMS and Wnt agonist 1, n = 4), sham + antagonist group (treated with XAV939, n = 4), and low-frequency + antagonist group (treated with rMS and XAV939, n = 4). (A) CCK-8 assay of the *in vitro* neuroblastoma model treated with vehicle, low-frequency rMS, agoinst, and/or antagoinst. (B) Quantification of CCK-8 assay. (C) CFA of the *in vitro* neuroblastoma model treated with vehicle, low-frequency rMS, agonist, and/or antagonist. (D) Quantification of CFA. (E) The relative gene expression of WNT3a, WNT5a, β-catenin, DVL1, and LEF1 detected by RT-qPCR. (F) Western blot analysis of the Wnt/β-catenin signaling pathway in the *in vitro* neuroblastoma model treated with vehicle, low-frequency rMS treatment, agonist, and/or antagonist. (G) Quantification of Western blot signals for the Wnt/β-catenin signaling pathway. (H) The relative gene expression of Bax and Bcl-2 detected by RT-qPCR. (I) Western blot analysis of Bax and Bcl-2 in the *in vitro* neuroblastoma model treated with vehicle, low-frequency rMS treatment, agonist, and/or antagonist. (J) Quantification of Western blot signals of Bax and Bcl-2 (K) TUNEL assay in the *in vitro* neuroblastoma model treated with vehicle, low-frequency rMS treatment, agonist, and/or antagonist. (L) Quantification of TUNEL assay. Values are presented as means ± SEM. Statistically significant differences are shown as *P < 0.05, **P < 0.01, ***P < 0.001.

CFA showed that Wnt agonist promoted cell proliferation, while Wnt antagonist suppressed cell growth. Moreover, the results showed that Wnt agonist reversed the ability of rMS to inhibit cell proliferation, while Wnt antagonist showed a similar effect on cell proliferation as rMS treatment (Fig. 3A-D).

Moreover, genes related to the Wnt/β-catenin signaling pathway, such as WNT3a, WNT5a, β-catenin, DVL1, and LEF1 were down-regulated in low-frequency + vehicle group compared to that in sham + vehicle group, while the expression of genes related to the Wnt/β-catenin signaling pathway was rescued in low-frequency + agonist group. The expression of these genes was downregulated in sham + antagoinst and low-frequency + antagonist groups compared to that in sham + vehicle group (Fig. 3E). Protein expression levels of WNT3a, WNT5a, β-catenin, DVL1, LEF1, cyclin D1, c-Myc, and phosphorylation of GSK3β were downregulated in low-frequency + vehicle group, while the expression of these proteins and phosphorylation of GSK3β were rescued in low-frequency + agonist group. The expression of these proteins and phosphorylation of GSK3β were downregulated in sham +

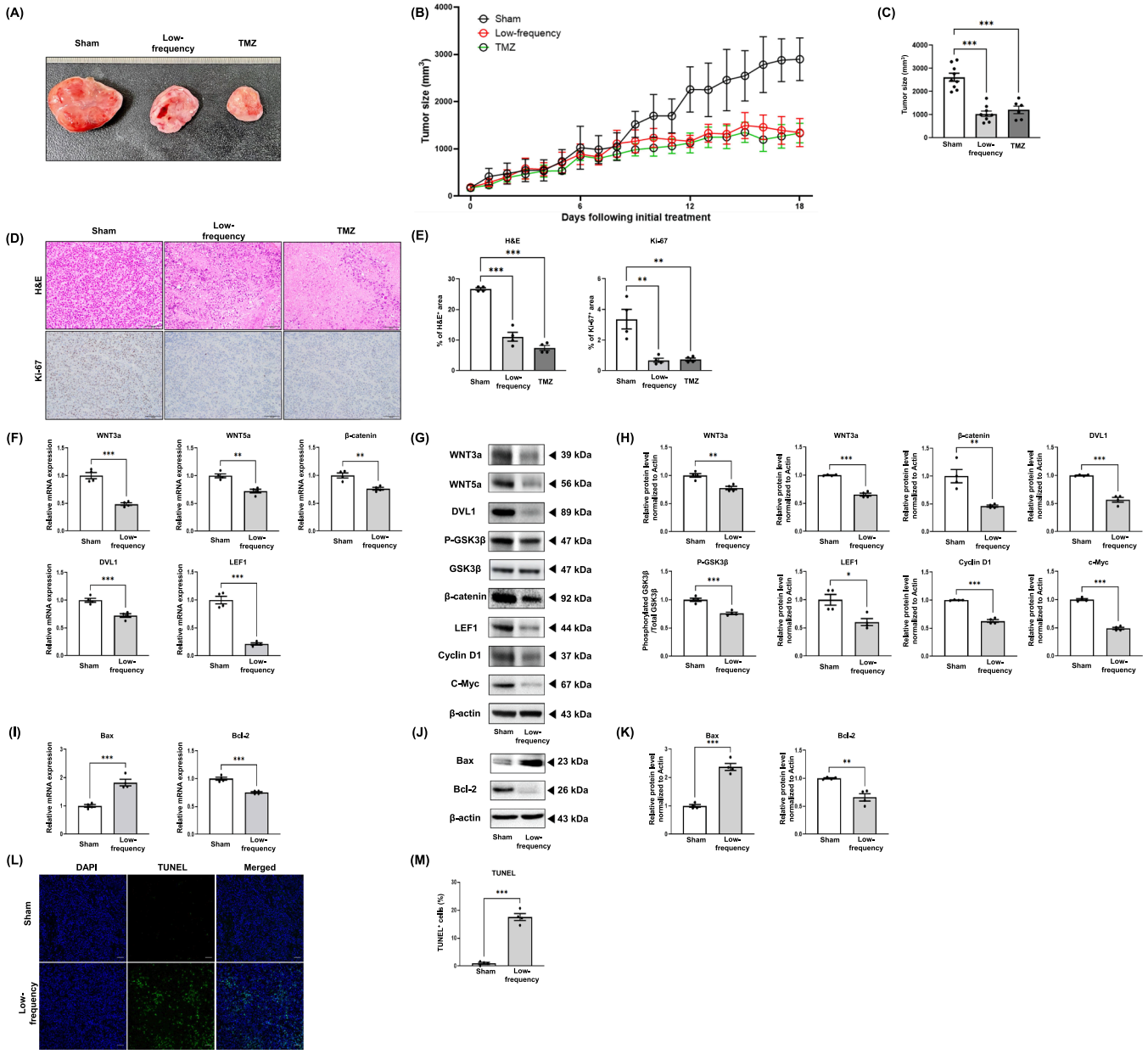

Fig. 4. Low-frequency rMS suppressed tumor progression in an *in vivo* neuroblastoma model. *In vivo* neuroblastoma model was divided into three groups: sham group (non-treated, n = 9), low-frequency group (treated with low-frequency rMS, n = 9), and TMZ group (treated with 30 mg/Kg temozolomide, n = 6). (A) Tumor volume of the *in vivo* neuroblastoma model treated with or without low-frequency rMS or TMZ. (B) Tumor progression of the *in vivo* neuroblastoma model treated with or without low-frequency rMS or TMZ. (C) Final tumor size of the *in vivo* neuroblastoma model treated with or without low-frequency rMS or TMZ. (D) Tumor tissue stained by Ki-67 antibody and H&E staining. (E) Quantification of cells stained with Ki-67 antibody and H&E staining. (F) Relative gene expression of WNT3a, WNT5a, β-catenin, DVL1, and LEF1 detected by RT-qPCR in the *in vivo* neuroblastoma model treated with or without low-frequency rMS. (G) Western blot analysis of the Wnt/β-catenin signaling pathway in the *in vivo* neuroblastoma model treated with or without low-frequency rMS (H) Quantification of Western blot signals for the Wnt/β-catenin signaling pathway (I) The relative gene expression of Bax and Bcl-2 detected by RT-qPCR (J) Western blot analysis of Bax and Bcl-2 in the *in vivo* neuroblastoma model treated with or without low-frequency rMS (K) Quantification of Western blot signals of Bax and Bcl-2 (L) TUNEL assay in the *in vivo* neuroblastoma model treated with or without low-frequency rMS (M) Quantification of TUNEL assay. Values are presented as means ± SEM. Scale bars = 100 μm. Statistically significant differences are shown as *P < 0.05, **P < 0.01, ***P < 0.001.

antagoinst and low-frequency + antagonist groups compared to that in sham + vehicle group (Fig. 3F-G). In addition, the expression gene and protein levels of Bcl-2 were downregulated in low-frequency + vehicle group compared to that in sham + vehicle group, while the expression gene and protein levels of Bcl-2 were rescued in low-frequency + agonist group. The expression levels of Bcl-2 were downregulated in sham + antagoinst and low-frequency + antagonist groups compared to that in sham + vehicle group. Meanwhile, the expression gene and protein levels of Bax showed the opposite trend to that of Bcl-2 (Fig. 3H-J). TUNEL positive cells were increased in low-frequency + vehicle, sham + antagonist, and low-frequency + antagonist groups compared to that in sham + vehicle group (Fig. 3K-L). These results revealed that low-frequency rMS inhibited cell proliferation in the *in vitro* neuroblastoma model by regulating the Wnt/β-catenin signaling pathway.

3.4. Low-frequency rMS suppresses tumor progression via downregulating the Wnt/β-catenin signaling pathway in an in vivo neuroblastoma model

To investigate the effects of low-frequency rMS in an *in vivo* neuroblastoma model, 5×10^6 N2a cells were injected into nude mice. Tumor progression was monitored and measured daily. Low-frequency group was treated with low-frequency rMS for 10 min each day. TMZ group was administered temozolomide, which is used as a positive control for the tumor suppression effect in neuroblastoma. Compared to sham group, low-frequency and TMZ groups exhibited significantly reduced tumor growth (Fig. 4A-C). To investigate differential tumor growth among other groups, sectioned tumor tissues were stained with Ki-67 antibody and H&E. There were fewer cells with Ki-67 antibody and H&E staining in the tumors of low-frequency and TMZ groups compared to that in sham group (Fig. 4D-E). The results demonstrated that low-freqeuncy rMS exerted a tumor suppression effect in the *in vivo* neuroblastoma model.

To elucidate the role of low-frequency rMS on the Wnt/β-catenin signaling pathway and apoptosis in the *in vivo* neuroblastoma model, RT-qPCR, Western blot, and TUNEL assay were conducted. Genes related to the Wnt/β-catenin signaling pathway, such as WNT3a, WNT5a, β-catenin, DVL1, and LEF1 were downregulated in low-frequency group compared to that in sham group (Fig. 4F). Protein expression levels of WNT3a, WNT5a, β-catenin, DVL1, LEF1, cyclin D1, and c-Myc were downregulated in low-frequency group compared to that in sham group. Phosphorylation of GSK3β was downregulated in low-frequency group compared to that in sham group (Fig. 4G-H). In addition, the expression gene and protein levels of Bcl-2 were downregulated after low-frequency rMS while the expression levels of Bax were upregulated (Fig. 4I-K). Moreover, TUNEL positive cells were increased in low-frequency group compared to that in sham group (Fig. 4L-M).

Next, we determined the effect of low-frequency rMS on the Wnt/β-catenin signaling pathway and apoptosis in the *in vivo* neuroblastoma model, using Wnt agonist and antagonist. Like the *in vitro* experiment, the *in vivo* neuroblastoma model was divided into six groups. The results of tumor size for each group showed that Wnt agonist promoted tumor progression, while Wnt antagonist suppressed tumor progression. In addition, the results revealed that Wnt agonist reversed the ability of rMS to inhibit tumor progression. Moreover, the effect of Wnt antagonist on tumor growth was similar to that of low-frequency rMS treatment (Fig. 5A-C). Sectioned tumor tissues were stained with LEF1, DVL1 antibodies, and H&E and there were fewer cells stained with LEF1, DVL1 antibodies, and H&E in the tumors of low-frequency + vehicle group compared to that in sham + vehicle group. However, these were rescued in low-frequency + agonist group. In addition, cells were less stained in sham + antagoinst and low-frequency + antagonist groups than in sham + vehicle group (Fig. 5D-E). Genes related to the Wnt/β-catenin signaling pathway, such as WNT3a, WNT5a, β-catenin, DVL1, and LEF1 were downregulated in low-frequency + vehicle group compared to that in sham + vehicle group, but the expression of these genes was rescued in low-frequency + agonist group. The genes were downregulated in sham + antagoinst and low-frequency + antagonist groups compared to that in sham + vehicle group (Fig. 5F). The expression of WNT3a, WNT5a, β-catenin, DVL1, LEF1, cyclin D1, c-Myc, and phosphorylation of GSK3β were downregulated in low-frequency + vehicle group, whereas the expression of proteins and phosphorylation of GSK3β were rescued in low-frequency + agonist group. The expression of these proteins and phosphorylation of GSK3β were downregulated in sham + antagoinst and low-frequency + antagonist groups compared to that in sham + vehicle group (Fig. 5G-H). In addition, the expression gene and protein levels of Bcl-2 were downregulated in low-frequency + vehicle group compared to that in sham + vehicle group, while the expression gene and protein levels of Bcl-2 were rescued in low-frequency + agonist group. The expression levels of Bcl-2 were downregulated in sham + antagoinst and low-frequency + antagonist groups compared to that in sham + vehicle group. However, the expression gene and protein levels of Bax showed the opposite trend to that of Bcl-2 (Fig. 5I-K). TUNEL positive cells were increased in low-frequency + vehicle, sham + antagonist, and low-frequency + antagonist groups compared to that in sham + vehicle group (Fig. 5L-M). These results showed that low-frequency rMS suppressed the tumor progression by downregulating the Wnt/β-catenin signaling pathway in the *in vivo* neuroblastoma model.

4. Discussion

rMS is a non-invasive and less painful treatment with no side effects. Many studies tried to utilize rMS as a therapy for various neurological disorders [3]. However, our group tried to use rMS as a cancer therapy. In previous study, we demonstrated that low-frequency rMS has an effect on the suppression of cell proliferation [26]. Therefore, our group explored a potential of low-frequency rMS as a cancer treatment by investigating the tumor suppression effect of low-frequency rMS in *in vitro* and *in vivo* neuroblastoma models, and the mechanism of low-frequency rMS.

In this study, the effect of low-frequency rMS on neuroblastoma was evaluated by the CCK-8 assay and CFA in the *in vitro* neuroblastoma model. The proliferation of neuroblastoma cells was significantly inhibited by low-frequency rMS. Moreover, biological mechanisms related to neuroblastoma progression, such as the JNK/p38/ERK and PI3K/AKT/mTOR pathways, were suppressed by low-frequency rMS (Fig. 1). Consistent with previous studies to compare the effect of rMS depending on the stimulation frequency, the results of the present study indicated that low-frequency rMS with 0.5 Hz may potentially inhibit cell proliferation of neuroblastoma and induce apoptosis in the *in vitro* neuroblastoma model [26–28].

To investigate the underlying biological mechanism of low-frequency rMS on neuroblastoma, we performed RNA-seq transcriptome analysis between sham group and low-frequency group of *in vitro* neuroblastoma model. GO analyses of biological processes using DAVID software indicated that the Wnt/β-catenin signaling pathway, which is highly related to neuroblastoma proliferation [40], was significantly downregulated in low-frequency group compared to that in sham group. The results of RT-qPCR and Western blot showed that low-frequency rMS regulated the Wnt/β-catenin signaling pathway. Recent studies have shown that the Wnt/β-catenin signaling pathway orchestrates many cell signaling pathways including the Notch, sonic hedgehog, nuclear factor kappa-B (NF-κB), and PI3K/AKT/mTOR pathways, which are important in tumor development [41]. Moreover, many studies demonstrated that the inhibition of the Wnt/β-catenin signaling pathway induces apoptosis and suppresses cell proliferation in many types of cancer [42–44]. Therefore, many treatments have been developed to target the genetic and epigenetic deregulation of the Wnt/β-catenin signaling pathway as neuroblatoma therapies [38,45]. Based on the results of the suppressive effect of low-frequency rMS on Wnt/β-catenin signaling pathway and PI3K/AKT/mTOR pathway related to

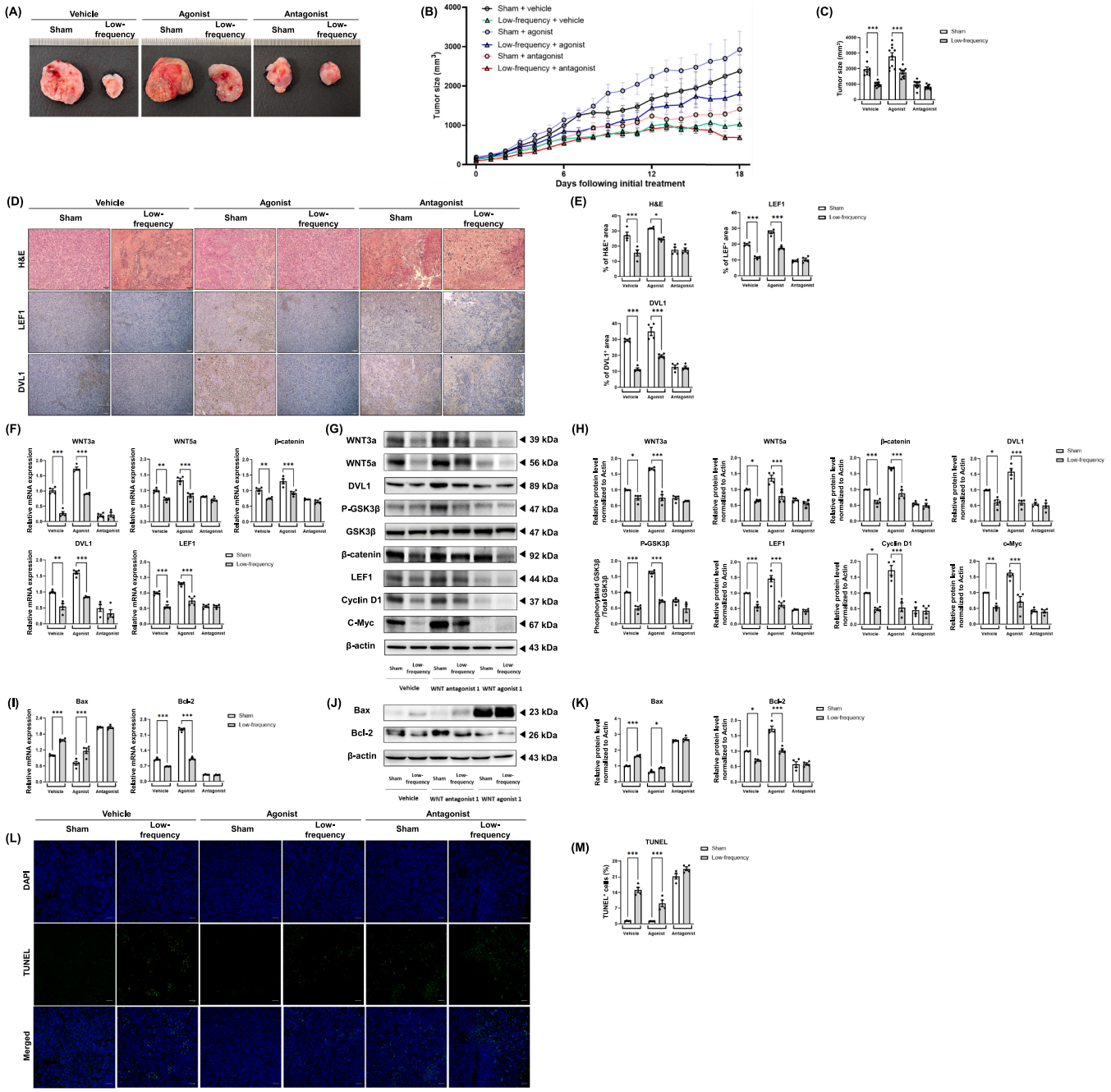

Fig. 5. Agonist and antagonist of the Wnt/β-catenin signaling pathway validated the effect of low-frequency rMS on the Wnt/β-catenin signaling pathway. The model was divided into six groups: sham + vehicle group (treated with PBS, n = 10), low-frequency + vehicle group (treated with rMS and PBS, n = 10), sham + agonist group (treated with Wnt agonist 1, n = 10), low-frequency + agonist group (treated with rMS and Wnt agonist 1, n = 10), sham + antagonist group (treated with XAV939, n = 10), and low-frequency + antagonist group (treated with rMS and XAV939, n = 10). (A) Tumor volume in the *in vivo* neuroblastoma model treated with vehicle, low-frequency rMS, agonist, and/or antagonist. (B) Tumor progression in the *in vivo* neuroblastoma model treated with vehicle, low-frequency rMS treatment, agoinst, and/or antagoinst. (C) Final tumor size of the *in vivo* neuroblastoma model treated with vehicle, low-frequency rMS treatment, agonist, and/or antagonist. (D) Tumor tissue stained by LEF1, DVL1 antibodies and H&E staining. (E) Quantification of cells stained with LEF1, DVL1 antibodies and H&E staining. (F) Relative gene expression of WNT3a, WNT5a, β-catenin, DVL1, and LEF1 detected by RT-qPCR in the *in vivo* neuroblastoma model treated with vehicle, low-frequency rMS treatment, agonist, and/or antagonist. (G) Western blot analysis of the Wnt/β-catenin signaling pathway in the *in vivo* neuroblastoma model treated with vehicle, low-frequency rMS treatment, agonist, and/or antagonist. (H) Quantification of Western blot signals for the Wnt/β-catenin signaling pathway (I) The relative gene expression of Bax and Bcl-2 detected by RT-qPCR (J) Western blot analysis of Bax and Bcl-2 in the *in vivo* neuroblastoma model treated with vehicle, low-frequency rMS treatment, agonist, and/or antagonist. (K) Quantification of Western blot signals of Bax and Bcl-2 (L) TUNEL assay in the *in vivo* neuroblastoma model treated with vehicle, low-frequency rMS treatment, agonist, and/or antagonist. (M) Quantification of TUNEL assay. Values are presented as means ± SEM. Scale bars = 100 μm. Statistically significant differences are shown as *P < 0.05, **P < 0.01, ***P < 0.001.

apoptosis [42,46], we investigated the effect of low-frequency rMS on apoptotic markers in neuroblastoma models. When the expression of Bax and Bcl-2 and TUNEL positive cells were compared between sham group and low-frequency group, the results demonstrated that low-frequency rMS induced apoptosis in the *in vitro* neuroblastoma model. This indicated that low-frequency rMS may have a suppression effect on cell proliferation of neuroblastoma and induce apoptosis by downregulating the Wnt/β-catenin signaling pathway (Fig. 2).

To further explanation, our group used Wnt agonist and antagonist to validate that low-frequency rMS regulates the Wnt/β-catenin signaling pathway in neuroblastoma. While Wnt antagonist significantly downregulated cell proliferation of neuroblastoma and the expression of genes and proteins related to the Wnt/β-catenin signaling pathway, Wnt agoinst significantly upregulated cell proliferation and the expression of genes and proteins. Furthermore, cell proliferation and the expression of genes and proteins, which were downregulated by low-frequency rMS, were rescued by Wnt agonist. In addition, the results demonstrated that the expression of genes and proteins of apoptosis and TUNEL positive cells in low-frequency + vehicle group and sham + antagonist group were similar. These results indicated that Wnt antagonist and low-frequency rMS have a similar effect in terms of regulating the Wnt/β-catenin signaling pathway and inducing apoptosis in the *in vitro* neuroblastoma model (Fig. 3).

Moreover, we used the *in vivo* neuroblastoma model to elucidate the effect of low-frequency rMS in an animal model, wherein we administered low-frequency rMS for 18 d. While sham group showed continued tumor progression until the end point, low-frequency group and TMZ group, which is the positive control group, exhibited lower tumor progression rates than sham group. As the tumor size (y) was plotted as days of low-frequency rMS treatment (x), simple regression analysis revealed that tumor progression of the *in vivo* neuroblastoma model in low-frequency group could be described by the line $y = 58.586x + 377.61$. By calculating tumor progression with the formula, tumor mass of low-frequency group may reach the volume of 3000 m^3 approximately 44 days after initial treatment. This indicated that low-frequency rMS delays the tumor growth of the *in vivo* neuroblastoma model since the tumor mass of sham group reached the volume of 3000 m^3 on 18 days. In addition, Ki-67, which is a representative marker of the tumor growth, was decreased and TUNEL positive cells were increased in low-frequency group and TMZ group compared to that in sham group (Fig. 4). Moreover, the effect of Wnt antagonist was similar to that of low-frequency rMS treatment on tumor progression and the expression of genes and proteins related to the Wnt/β-catenin signaling pathway and apoptosis in the *in vivo* neuroblastoma model, whereas Wnt agonist counteracted the effect of low-frequency rMS treatment in the *in vivo* neuroblastoma model. These results indicated that low-frequency rMS reduced tumor progression and induced apoptosis via downregulating the Wnt/β-catenin signaling pathway in the *in vivo* neuroblastoma model (Fig. 5).

Recently, several groups have explored rMS as a less toxic and more effective treatment for cancer therapy, but most of these studies focused on relatively high-frequency or ultra-high-frequency rMS [24,47]. There are few studies that have suggested low intensity and frequency pulsed MS has the potential to treat some types of cancers [25,48]. Recent studies demonstrated that pulsed low-frequency MS induces the growth arrest and metabolic shift in malignant mesothelioma and increases DNA damage and caspase-dependent apoptotic pathways by upregulating the intracellular ROS in breast cancer cells [49,50]. Several protocols of MS were suggested for cancer treatment, however, the intensity, frequency, and duration of stimulation were varied [47–51]. Based on parameters of preclinical and clinical application protocols of rMS [12], previous studies conducted the research focusing on the frequency to compare differential effects of rMS and identified that high-frequency rMS increased cell proliferation in neuroblastoma, whereas low-frequency rMS showed a suppressive effect on the cell proliferation [27,28]. Similar intensity of stimulation elucidated the effectiveness on the inhibition of cell proliferation of glioma (18 mT) [51]. Even though the frequency set of the stimulation in this study (0.5 Hz) was not reported to utilize for cancer treatment, the results demonstrated that low-frequency rMS downregulated neuroblastoma progression via the Wnt/β-catenin signaling pathway. Therefore, it may be possible to utilize low-frequency rMS may have potential as a therapy for neuroblastoma. However, further research will be required to elucidate a dosimetric quantification of low-frequency rMS in varied stimulation frequencies, intensities and exposure times on neuroblastoma models and the underlying biological mechanisms of low-frequency rMS in other types of cancer. Moreover, it will be necessary to establish rMS to target the exact site of tumor mass for future clinical applications in order to avoid the side effect of low-frequency rMS on the healthy tissue.

5. Conclusion

In summary, our findings suggested that low-frequency rMS may suppress the progression of neuroblastoma via the Wnt/β-catenin signaling pathway. These results indicate that the potential benefits of low-frequency rMS in neuroblastoma. Therefore, the present study provides academic evidence to establish low-frequency rMS as a future therapeutic strategy for neuroblastoma treatment.

CRediT authorship contribution statement

Seongmoon Jo: Conceptualization, Data curation, Formal analysis, Funding acquisition, Investigation, Methodology, Validation, Visualization, Writing – original draft, Writing – review & editing. **Sang Hee Im:** Funding acquisition, Investigation, Project administration, Resources, Supervision, Validation. **Dongryul Seo:** Data curation, Investigation, Methodology, Validation. **Hayeon Ryu:** Data curation, Investigation, Methodology, Validation. **Sung Hoon Kim:** Conceptualization, Funding acquisition, Investigation, Project administration, Resources, Supervision, Validation. **Dawoon Baek:** Data curation, Investigation, Methodology, Validation. **Ahreum Baek:** Conceptualization, Data curation, Formal analysis, Funding acquisition, Investigation, Methodology, Project administration, Supervision, Validation, Visualization, Writing – original draft, Writing – review & editing. **Sung-Rae Cho:** Conceptualization, Data curation, Formal analysis, Funding acquisition, Investigation, Methodology, Supervision, Validation, Visualization, Writing – original draft, Writing – review & editing.

Declaration of Competing Interest

The authors declare that they have no known competing financial interests or personal relationships that could have appeared to influence the work reported in this paper.

Acknowledgements

The authors thank Medical Illustration & Design, part of the Medical Research Support Services of Yonsei University College of Medicine, for all artistic support related to this work. In addition, we would like to thank Editage (www.editage.co.kr) for English language editing.

Funding

This study was supported by the National Research Foundation (NRF-2020R1A2C1012019, 2022R1A2C1006660, and 2022R1A2C 1006374), the faculty research grant of Yonsei University College of Medicine (6-2021-0095), the Korean Fund for Regenerative Medicine (KFRM) grant funded by the Korea government (the Ministry of Science and ICT, the Ministry of Health & Welfare) (21A0202L1), and the grant from Hyundai Motor Chung Mong-Koo Foundation.

Appendix A. Supplementary material

Supplementary data to this article can be found online at https://doi.org/10.1016/j.bioelechem.2022.108205.

References

[1] A.T. Barker, R. Jalinous, I.L. Freeston, Non-invasive magnetic stimulation of human motor cortex, Lancet 1 (1985) 1106–1107.
[2] M.R. Ljubisavljevic, A. Javid, J. Oommen, K. Parekh, N. Nagelkerke, S. Shehab, T. E. Adrian, The effects of different repetitive transcranial magnetic stimulation (rTMS) protocols on cortical gene expression in a rat model of cerebral ischemic-reperfusion injury, PLoS ONE 10 (2015), e0139892.
[3] M. Kobayashi, A. Pascual-Leone, Transcranial magnetic stimulation in neurology, Lancet Neurol. 2 (2003) 145–156.
[4] T.E. Schlaepfer, M. Kosel, C.B. Nemeroff, Efficacy of repetitive transcranial magnetic stimulation (rTMS) in the treatment of affective disorders, Neuropsychopharmacology 28 (2003) 201–205.
[5] J. Li, X.M. Meng, R.Y. Li, R. Zhang, Z. Zhang, Y.F. Du, Effects of different frequencies of repetitive transcranial magnetic stimulation on the recovery of upper limb motor dysfunction in patients with subacute cerebral infarction, Neural Regen. Res. 11 (2016) 1584–1590.
[6] K.A. Bates, J. Rodger, Repetitive transcranial magnetic stimulation for stroke rehabilitation-potential therapy or misplaced hope? Restor. Neurol. Neurosci. 33 (2015) 557–569.
[7] H.K. Kim, D.M. Blumberger, J. Downar, Z.J. Daskalakis, Systematic review of biological markers of therapeutic repetitive transcranial magnetic stimulation in neurological and psychiatric disorders, Clin. Neurophysiol. 132 (2021) 429–448.
[8] R.G. Monem, O.O. Okusaga, Repetitive transcranial magnetic stimulation: a potential treatment for obesity in patients with schizophrenia, Behav. Sci.-Basel 11 (2021).
[9] S.M. McClintock, E. Kallioniemi, D.M. Martin, J.U. Kim, S.L. Weisenbach, C. C. Abbott, A critical review and synthesis of clinical and neurocognitive effects of noninvasive neuromodulation antidepressant therapies, Focus (Am. Psychiatr. Publ.) 17 (2019) 18–29.
[10] E. Houdayer, A. Degardin, F. Cassim, P. Bocquillon, P. Derambure, H. Devanne, The effects of low- and high-frequency repetitive TMS on the input/output properties of the human corticospinal pathway, Exp. Brain Res. 187 (2008) 207–217.
[11] B.R. Kim, M.H. Chun, D.Y. Kim, S.J. Lee, Effect of high- and low-frequency repetitive transcranial magnetic stimulation on visuospatial neglect in patients with acute stroke: a double-blind, sham-controlled trial, Arch. Phys. Med. Rehabil. 94 (2013) 803–807.
[12] E.M. Wassermann, S.H. Lisanby, Therapeutic application of repetitive transcranial magnetic stimulation: a review, Clin. Neurophysiol. 112 (2001) 1367–1377.
[13] S.B. Whittle, V. Smith, E. Doherty, S. Zhao, S. McCarty, P.E. Zage, Overview and recent advances in the treatment of neuroblastoma, Expert Rev. Anticancer Ther. 17 (2017) 369–386.
[14] K.K. Matthay, J.M. Maris, G. Schleiermacher, A. Nakagawara, C.L. Mackall, L. Diller, W.A. Weiss, Neuroblastoma, Nat. Rev. Dis. Primers 2 (2016) 16078.
[15] J.R. Park, R. Bagatell, W.B. London, J.M. Maris, S.L. Cohn, K.K. Mattay, M. Hogarty, C.O.G.N. Committee, Children's Oncology Group's 2013 blueprint for research: neuroblastoma, Pediatr Blood Cancer 60 (2013) 985–993.
[16] L.M. Wagner, M.K. Danks, New therapeutic targets for the treatment of high-risk neuroblastoma, J. Cell Biochem. 107 (2009) 46–57.
[17] P.E. Zage, M. Kletzel, K. Murray, R. Marcus, R. Castleberry, Y. Zhang, W.B. London, C. Kretschmar, G. Children's oncology, outcomes of the POG 9340/9341/9342 trials for children with high-risk neuroblastoma: a report from the Children's Oncology Group, Pediatr. Blood Cancer 51 (2008) 747–753.
[18] J.W. Lin, J.T. Chen, C.Y. Hong, Y.L. Lin, K.T. Wang, C.J. Yao, G.M. Lai, R.M. Chen, Honokiol traverses the blood-brain barrier and induces apoptosis of neuroblastoma cells via an intrinsic bax-mitochondrion-cytochrome c-caspase protease pathway, Neuro-Oncology 14 (2012) 302–314.
[19] M. Attia, D. McCarthy, M. Abdelghani, Repetitive transcranial magnetic stimulation for treating chronic neuropathic pain: a systematic review, Curr. Pain Headache Rep. 25 (2021) 48.
[20] J. Nizard, A. Levesque, N. Denis, E. de Chauvigny, A. Lepeintre, S. Raoul, J. J. Labat, S. Bulteau, B. Maillard, K. Buffenoir, G. Potel, J.P. Lefaucheur, J. P. Nguyen, Interest of repetitive transcranial magnetic stimulation of the motor cortex in the management of refractory cancer pain in palliative care: two case reports, Palliat. Med. 29 (2015) 564–568.
[21] J. Ruohonen, J. Karhu, Navigated transcranial magnetic stimulation, Neurophysiol. Clin. 40 (2010) 7–17.
[22] N. Sollmann, S. Ille, T. Hauck, S. Maurer, C. Negwer, C. Zimmer, F. Ringel, B. Meyer, S.M. Krieg, The impact of preoperative language mapping by repetitive navigated transcranial magnetic stimulation on the clinical course of brain tumor patients, BMC Cancer 15 (2015) 261.
[23] S. Ille, K. Drummer, K. Giglhuber, N. Conway, S. Maurer, B. Meyer, S.M. Krieg, Mapping of arithmetic processing by navigated repetitive transcranial magnetic stimulation in patients with parietal brain tumors and correlation with postoperative outcome, World Neurosurg. 114 (2018) e1016–e1030.
[24] S. Yamaguchi, M. Ogiue-Ikeda, M. Sekino, S. Ueno, Effects of pulsed magnetic stimulation on tumor development and immune functions in mice, Bioelectromagnetics 27 (2006) 64–72.
[25] C.P. Ashdown, S.C. Johns, E. Aminov, M. Unanian, W. Connacher, J. Friend, M. M. Fuster, Pulsed low-frequency magnetic fields induce tumor membrane disruption and altered cell viability, Biophys. J. 118 (2020) 1552–1563.
[26] J.Y. Lee, H.J. Park, J.H. Kim, B.P. Cho, S.R. Cho, S.H. Kim, Effects of low- and high-frequency repetitive magnetic stimulation on neuronal cell proliferation and growth factor expression: a preliminary report, Neurosci. Lett. 604 (2015) 167–172.
[27] A. Baek, J.H. Kim, S. Pyo, J.H. Jung, E.J. Park, S.H. Kim, S.R. Cho, The differential effects of repetitive magnetic stimulation in an in vitro neuronal model of ischemia/reperfusion injury, Front. Neurol. 9 (2018) 50.
[28] A. Baek, E.J. Park, S.Y. Kim, B.G. Nam, J.H. Kim, S.W. Jun, S.H. Kim, S.R. Cho, High-frequency repetitive magnetic stimulation enhances the expression of brain-derived neurotrophic factor through activation of Ca2+-calmodulin-dependent protein kinase II-cAMP-response element-binding protein pathway, Front. Neurol. 9 (2018).
[29] S.J. Yu, L. Li, K.L. Fan, Y.D. Li, Y. Gao, A genome-scale CRISPR knock-out screen identifies MicroRNA-5197-5p as a promising radiosensitive biomarker in colorectal cancer, Front. Oncol. 11 (2021).
[30] P. Chomczynski, A reagent for the single-step simultaneous isolation of RNA, DNA and proteins from cell and tissue samples, Biotechniques 15 (532–534) (1993) 536–537.
[31] A. Baek, M. Kim, S. Kim, S.R. Cho, H. Kim, Anti-inflammatory effect of DNA polymeric molecules in a cell model of osteoarthritis, Inflammation 41 (2018) 677–688.
[32] A. Tomczak, J.M. Mortensen, R. Winnenburg, C. Liu, D.T. Alessi, V. Swamy, F. Vallania, S. Lofgren, W. Haynes, N.H. Shah, M.A. Musen, P. Khatri, Interpretation of biological experiments changes with evolution of the Gene Ontology and its annotations, Sci. Rep. 8 (2018) 5115.
[33] M. Fan, R.F. Mi, D.T. Yew, W.Y. Chan, Analysis of gene expression following sciatic nerve crush and spinal cord hemisection in the mouse by microarray expression profiling, Cell Mol. Neurobiol. 21 (2001) 497–508.
[34] M. Lenz, C. Galanis, F. Muller-Dahlhaus, A. Opitz, C.J. Wierenga, G. Szabo, U. Ziemann, T. Deller, K. Funke, A. Vlachos, Repetitive magnetic stimulation induces plasticity of inhibitory synapses, Nat. Commun. 7 (2016) 10020.
[35] C. Zhang, R. Lu, L. Wang, W. Yun, X. Zhou, Restraint devices for repetitive transcranial magnetic stimulation in mice and rats, Brain Behav. 9 (2019), e01305.
[36] D. King, D. Yeomanson, H.E. Bryant, PI3King the lock: targeting the PI3K/Akt/mTOR pathway as a novel therapeutic strategy in neuroblastoma, J. Pediat. Hematol. Onc. 37 (2015) 245–251.
[37] T. Xiang, R.S. Fei, Z. Wang, Z.L. Shen, J. Qian, W.B. Chen, Nicotine enhances invasion and metastasis of human colorectal cancer cells through the nicotinic acetylcholine receptor downstream p38 MAPK signaling pathway, Oncol. Rep. 35 (2016) 205–210.
[38] J.N. Anastas, R.T. Moon, WNT signalling pathways as therapeutic targets in cancer, Nat. Rev. Cancer 13 (2013) 11–26.
[39] J. Song, C. Xie, L. Jiang, G. Wu, J. Zhu, S. Zhang, M. Tang, L. Song, J. Li, Transcription factor AP-4 promotes tumorigenic capability and activates the Wnt/beta-catenin pathway in hepatocellular carcinoma, Theranostics 8 (2018) 3571–3583.
[40] J. Becker, J. Wilting, WNT signaling in neuroblastoma, Cancers (Basel) 11 (2019).
[41] Y. Zhang, X. Wang, Targeting the Wnt/beta-catenin signaling pathway in cancer, J. Hematol. Oncol. 13 (2020) 165.
[42] X.H. Tian, W.J. Hou, Y. Fang, J. Fan, H. Tong, S.L. Bai, Q. Chen, H. Xu, Y. Li, XAV939, a tankyrase 1 inhibitior, promotes cell apoptosis in neuroblastoma cell lines by inhibiting Wnt/beta-catenin signaling pathway, J. Exp. Clin. Cancer Res. 32 (2013) 100.
[43] B. Bilir, O. Kucuk, C.S. Moreno, Wnt signaling blockage inhibits cell proliferation and migration, and induces apoptosis in triple-negative breast cancer cells, J. Transl. Med. 11 (2013) 280.
[44] K.S. Zhang, Q. Zhou, Y.F. Wang, L.J. Liang, Inhibition of Wnt signaling induces cell apoptosis and suppresses cell proliferation in cholangiocarcinoma cells, Oncol. Rep. 30 (2013) 1430–1438.
[45] I. Spaan, R.A. Raymakers, A. van de Stolpe, V. Peperzak, Wnt signaling in multiple myeloma: a central player in disease with therapeutic potential, J. Hematol. Oncol. 11 (2018) 67.
[46] Z. Zou, T. Tao, H. Li, X. Zhu, mTOR signaling pathway and mTOR inhibitors in cancer: progress and challenges, Cell Biosci. 10 (1) (2020) 31-31, https://doi.org/10.1186/s13578-020-00396-1, in this issue.
[47] S. Sengupta, V.K. Balla, A review on the use of magnetic fields and ultrasound for non-invasive cancer treatment, J. Adv. Res. 14 (2018) 97–111.
[48] S. Crocetti, C. Beyer, G. Schade, M. Egli, J. Frohlich, A. Franco-Obregon, Low intensity and frequency pulsed electromagnetic fields selectively impair breast cancer cell viability, PLoS ONE 8 (2013), e72944.
[49] L. Bergandi, U. Lucia, G. Grisolia, R. Granata, I. Gesmundo, A. Ponzetto, E. Paolucci, R. Borchiellini, E. Ghigo, F. Silvagno, The extremely low frequency electromagnetic stimulation selective for cancer cells elicits growth arrest through a metabolic shift, Bba-Mol. Cell Res. 2019 (1866) 1389–1397.
[50] S.H. Woo, B. Kim, S.H. Kim, B.C. Jung, Y. Lee, Y.S. Kim, Pulsed electromagnetic field potentiates etoposide-induced MCF-7 cell death, BMB Rep. 55 (2022) 148–153.
[51] W. Xu, J. Sun, Y. Le, J. Chen, X. Lu, X. Yao, Effect of pulsed millisecond current magnetic field on the proliferation of C6 rat glioma cells, Electromagn. Biol. Med. 38 (2019) 185–197.